

## Electron Spin Resonance Studies on Bis(dimethylglyoximato)cobalt(II) and its Complexes with Pyridine

By Antal Rockenbauer,\* Éva Budó-Záhonyi, and László I. Simándi, Central Research Institute for Chemistry, Hungarian Academy of Sciences, Budapest, Hungary

The e.s.r. spectra of bis(dimethylglyoximato)cobalt(II) and its pyridine complexes have been studied in methanol. The spectra obtained in both liquid and frozen methanol show the existence of three paramagnetic centres, viz.  $[\text{Co}(\text{Hdmg})_2]$ ,  $[\text{Co}(\text{Hdmg})_2(\text{py})]$ , and  $[\text{Co}(\text{Hdmg})_2(\text{py})_2]$  (Hdmg is the monoanion of dimethylglyoxime), and that of a diamagnetic adduct  $\{[\text{Co}(\text{Hdmg})_2(\text{py})]_2\}$ . The magnetic parameters have been determined for each paramagnetic species; a significant temperature dependence has been observed in the case of  $[\text{Co}(\text{Hdmg})_2]$ . The parameters indicate a low-spin  ${}^2A_1$  ground state. The Fermi-contact term for  $[\text{Co}(\text{Hdmg})_2]$  varies between  $-20.0 \times 10^{-4}$  and  $-10.5 \times 10^{-4} \text{ cm}^{-1}$  on decreasing the temperature from 62 °C to the freezing point of methanol; the values for  $[\text{Co}(\text{Hdmg})_2(\text{py})]$  and  $[\text{Co}(\text{Hdmg})_2(\text{py})_2]$  are  $-3.9 \times 10^{-4}$  and  $9.8 \times 10^{-4} \text{ cm}^{-1}$ , respectively, at liquid-nitrogen temperature. The observed trend is consistent with the variation in the axial ligand field, which affects the Fermi term through  $3d-4s$  mixing. The linewidth variation of the hyperfine multiplet in the e.s.r. spectrum of  $[\text{Co}(\text{Hdmg})_2]$  has been studied in methanol as a function of temperature. The widths of the strongly overlapping lines have been determined by an automatic-fitting procedure. Good simulation and rapid convergence have been obtained by assuming Lorentzian lineshapes. The predominant factors contributing to the linewidths are spin-rotational relaxation at high temperatures and anisotropic relaxation at low temperatures.

BIS(DIMETHYLGlyoximato)COBALT(II),  $[\text{Co}(\text{Hdmg})_2]$ , has been extensively studied as a vitamin B<sub>12r</sub> model compound.<sup>1</sup> On the basis of the e.s.r. spectra it has been established that vitamin B<sub>12r</sub> and  $[\text{Co}(\text{Hdmg})_2]$  have also similar magnetic properties: the cobalt ion is in the low-spin  ${}^2A_1$  state and the unpaired electron is localized mainly on the  $d_{z^2}$  orbital.<sup>2-4</sup> The axial localization of the unpaired electron permits the formation of various mixed-ligand complexes to be followed using the e.s.r. spectra. In an earlier paper<sup>5</sup> the e.s.r. spectra of liquid methanol solutions containing  $[\text{Co}(\text{Hdmg})_2]$  and varying amounts of pyridine (py) were studied. The results clearly pointed to the existence of 1:1 and 1:2 adducts of composition  $[\text{Co}(\text{Hdmg})_2(\text{py})_n]$  ( $n = 1$  or 2). The corresponding stability constants were determined. However, the e.s.r. spectra recorded in frozen solution led to the conclusion<sup>2,3</sup> that various nitrogen bases form only 1:2 adducts; it was not possible to detect the 1:1 adducts, because of extensive dimerization. There is some weak axial co-ordination even in non-co-ordinating solvents as shown by the solvent dependence of the magnetic parameters.<sup>2,3</sup>

The objective of this paper is the detection of the 1:1 complex,  $[\text{Co}(\text{Hdmg})_2(\text{py})]$ , in frozen solution and to determine the dimerization constant from the liquid-phase e.s.r. spectra. In addition to a study and interpretation of the magnetic parameters, we shall deal with the variation in linewidths in the liquid phase.

### RESULTS

*E.S.R. Spectra.*—In frozen methanol solution  $[\text{Co}(\text{Hdmg})_2]$  had a complex spectrum which changed slightly with the concentration and with the rate of cooling; therefore, we shall only deal with the interpretation of spectra obtained at low concentrations and rapid freezing. The spectra exhibited a nearly axial symmetry and a <sup>59</sup>Co hyperfine structure. Attempts at simulating the perpendicular part

<sup>1</sup> G. N. Schrauzer, *Accounts Chem. Res.*, 1968, **1**, 97; G. Costa, *Pure Appl. Chem.*, 1972, **30**, 335; A. Bigotto, G. Costa, G. Mestroni, G. Pellizer, A. Puxeddu, E. Reisenhofer, L. Stefani, and G. Tauzher, *Inorg. Chim. Acta Rev.*, 1970, **4**, 41; and refs. therein.

<sup>2</sup> G. N. Schrauzer and Lian-Pin Lee, *J. Amer. Chem. Soc.*, 1968, **90**, 6541.

of the spectrum were unsuccessful when taking into account a rhombic distortion,<sup>4</sup> quadrupole effect,<sup>6</sup> or 'extra' absorption. An adequate fit was obtained, however, between simulated and experimental spectra when variation in linewidths with the magnetic quantum number and orientation was permitted (Figure 1).

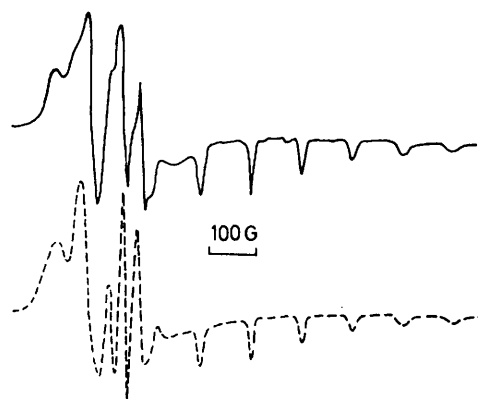


FIGURE 1 E.s.r. spectrum of  $[\text{Co}(\text{Hdmg})_2]$  in frozen methanol solution at 77 K. (—), Experimental; (---), calculated

On adding py to  $[\text{Co}(\text{Hdmg})_2]$  the form of the spectrum did not change until the concentration of py reached ca. 80% of that of the complex; however, the amplitude decreased with increasing py concentration. When the py :  $[\text{Co}(\text{Hdmg})_2]$  ratio exceeded 0.8 : 1 a 1:1:1 triplet superhyperfine structure appeared on the parallel hyperfine lines. At a ratio of 1.0 : 1 the triplet predominated although a 1:2:3:2:1 quintet also appeared. The above changes were most pronounced in the fourth parallel line (Figure 2). When the py concentration was greater than that of  $[\text{Co}(\text{Hdmg})_2]$  the 1:2:3:2:1 quintet became the predominant superhyperfine pattern. The overall intensity of the spectrum showed a characteristic dependence on

<sup>3</sup> E. K. Ivanova, I. N. Marov, A. T. Panfilov, O. M. Petruhin, and V. V. Zhukov, *Zhur. neorg. Khim.*, 1973, **18**, 1298.

<sup>4</sup> J. R. Pilbrow and M. E. Winfield, *Mol. Phys.*, 1973, **25**, 1073.

<sup>5</sup> A. Rockenbauer, É. Budó-Záhonyi, and L. I. Simándi, *J. Co-ordination Chem.*, 1972, **2**, 53.

<sup>6</sup> (a) F. D. Tsay, H. B. Gray, and J. Danon, *J. Chem. Phys.*, 1971, **54**, 3760; (b) L. D. Rollman and S. I. Chan, *ibid.*, 1969, **50**, 3416.

[py]. When the py : [Co(Hdmg)<sub>2</sub>] ratio was either zero or very large the overall signal intensity was the same, but at a ratio of 1.0 : 1 the intensity was at a minimum. At [Co(Hdmg)<sub>2</sub>]<sub>T</sub> = 10<sup>-2</sup> mol dm<sup>-3</sup> the minimum intensity was *ca.* 20 times smaller than at the maximum. The appearance of 1 : 1 : 1 and 1 : 2 : 3 : 2 : 1 superhyperfine structures confirms the existence of adducts with compositions [Co(Hdmg)<sub>2</sub>(py)] and [Co(Hdmg)<sub>2</sub>(py)<sub>2</sub>], and the observed intensity changes indicate dimerization of the five-co-ordinate complex in agreement with an earlier

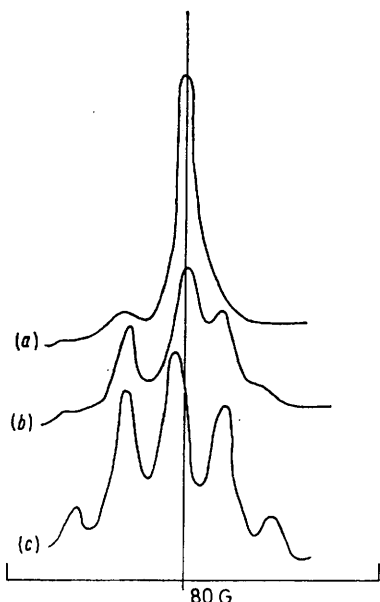


FIGURE 2 Part of the e.s.r. spectrum of the [Co(Hdmg)<sub>2</sub>]-py system in frozen methanol solution at 77 K. Fourth line of the cobalt hyperfine structure in parallel orientation: (a), [Co(Hdmg)<sub>2</sub>]; (b), [Co(Hdmg)<sub>2</sub>(py)]; (c), [Co(Hdmg)<sub>2</sub>(py)<sub>2</sub>]

report.<sup>7</sup> Values of the magnetic parameters obtained from the spectra of frozen solutions are listed in Table 1.

TABLE 1

E.s.r. parameters for the [Co(Hdmg)<sub>2</sub>]-pyridine system in methanol at 77 K

Adduct	<i>g</i> <sub>  </sub>	<i>g</i> <sub>⊥</sub>	<i>A</i> / 10 <sup>-4</sup> cm <sup>-1</sup>		
			<i>A</i> <sub>  Co</sub>	<i>A</i> <sub>⊥Co</sub>	<i>A</i> <sub>  N</sub>
[Co(Hdmg) <sub>2</sub> ]	2.0106	2.236	102.0	28.6	
[Co(Hdmg) <sub>2</sub> (py)]	2.0137	2.24 *	86.5	15.0 *	15.5
[Co(Hdmg) <sub>2</sub> (py) <sub>2</sub> ]	2.0161	2.205 *	78.0	9.0 *	15.8

\* Approximate estimation.

The solution spectra also support this conclusion. The e.s.r. spectrum of [Co(Hdmg)<sub>2</sub>] in methanol was an eight-line multiplet. The width of the hyperfine lines, the line separation, and the centre of the spectrum were strongly temperature dependent. Since the hyperfine lines overlapped considerably, a simulation procedure was used to determine the isotropic *g* values (*g*<sub>iso</sub>), the isotropic hyperfine constant (*A*<sub>iso</sub>), and the different widths of the eight lines. Spectra of samples containing various amounts of py consisted of three components, indicating the relatively long lifetimes of the mixed-ligand species [Co(Hdmg)<sub>2</sub>(py)] and [Co(Hdmg)<sub>2</sub>(py)<sub>2</sub>]. The iterative procedure described earlier<sup>5</sup> for the determination of the stepwise stability constants from e.s.r. data has now been modified so that, in

addition to *K*<sub>1</sub> and *K*<sub>2</sub>, the dimerization constant (if the extent of dimerization is significant) and the spectrum of each paramagnetic component can also be obtained, using e.s.r. spectra of six different solutions of suitable composition. The dependence of signal intensity on cobalt concentration shows that dimerization occurs only in the case of [Co(Hdmg)<sub>2</sub>(py)] according to the equation 2[Co(Hdmg)<sub>2</sub>(py)] ⇌ [(py)(Hdmg)<sub>2</sub>CoCo(Hdmg)<sub>2</sub>(py)]. For the definition of the stability constants see Table 2 in which the corresponding values are listed. Table 3 contains the isotropic magnetic parameters determined from the resolved spectra. For the *A*<sub>iso</sub> value of [Co(Hdmg)<sub>2</sub>(py)<sub>2</sub>] only an upper limit is given since its spectrum was a structureless singlet.

TABLE 2

Stability constants (dm<sup>3</sup> mol<sup>-1</sup>) of the [Co(Hdmg)<sub>2</sub>]-py systems in methanol

Method	θ <sub>c</sub> /°C	<i>K</i> <sub>1</sub>	<i>K</i> <sub>2</sub>	<i>K</i> <sub>d</sub>
E.s.r.	41	131 ± 20	0.58 ± 0.08	
E.s.r.	20	175 ± 30	0.83 ± 0.08	
E.s.r.	0	300 ± 60	1.52 ± 0.30	
E.s.r.	-30	853 ± 100	3.00 ± 0.4	2.4 ± 4
E.s.r.	-50	1 610 ± 200	7.34 ± 0.8	77.0 ± 10
Optical	r.t.	128	0.93	

*K*<sub>1</sub> = [Co(Hdmg)<sub>2</sub>(py)]/[Co(Hdmg)<sub>2</sub>][py], *K*<sub>2</sub> = [Co(Hdmg)<sub>2</sub>(py)<sub>2</sub>]/[Co(Hdmg)<sub>2</sub>(py)][py], and *K*<sub>d</sub> = {[Co(Hdmg)<sub>2</sub>(py)<sub>2</sub>]/[Co(Hdmg)<sub>2</sub>(py)]<sup>2</sup>.

TABLE 3

E.s.r. parameters and near-i.r. bands for the [Co(Hdmg)<sub>2</sub>]-py system in methanol at room temperature

Adduct	<i>g</i> <sub>iso</sub>	10 <sup>4</sup> <i>A</i> <sub>iso</sub> /cm <sup>-1</sup>	I.r. band (cm <sup>-1</sup> )
[Co(Hdmg) <sub>2</sub> ]	2.193	58.2	10 800
[Co(Hdmg) <sub>2</sub> (py)]	2.194	38.9	8 600, 11 200
[Co(Hdmg) <sub>2</sub> (py) <sub>2</sub> ]	2.142	≤ 20	13 500

**Electronic Absorption Spectra.**—Electronic absorption spectra were recorded at room temperature. The complex [Co(Hdmg)<sub>2</sub>] in methanol showed a weak asymmetric band in the near-i.r. region, a medium-intensity band and two shoulders in the visible, and strong charge-transfer (c.t.) bands in the u.v. region. The i.r. band appeared at 10 800 cm<sup>-1</sup> and the visible band at 21 200 cm<sup>-1</sup>. On adding py to the samples the positions of these bands varied. With increasing [py] the asymmetric i.r. band first split into two and the visible one showed a blue shift; at high [py] there was again one i.r. band (13 500 cm<sup>-1</sup>) and the visible band returned to 21 200 cm<sup>-1</sup>. By means of the electronic absorption spectra the stepwise stability constants (dimerization is negligible at room temperature) and the spectra of [Co(Hdmg)<sub>2</sub>(py)] and [Co(Hdmg)<sub>2</sub>(py)<sub>2</sub>] were determined with the same computer program as used in the analysis of the e.s.r. spectra. The stability constants obtained by the two methods were in fairly good agreement (*cf.* Table 2).

**Linewidth Measurements.**—The temperature dependence of the e.s.r. spectra of [Co(Hdmg)<sub>2</sub>] in methanol was studied in the interval between 62 and -60 °C. At 62 °C the spectrum was a broad symmetric singlet (Figure 3). On decreasing the temperature the eight-line hyperfine structure gradually appeared. The best resolution was obtained at *ca.* -20 °C (Figures 4 and 5). The linewidth increased on going to higher fields. At *ca.* -60 °C the lines collapsed into an asymmetric singlet (Figure 6).

<sup>7</sup> G. N. Schrauzer and R. J. Windgassen, *Chem. Ber.*, 1966, **99**, 602.

For determination of the linewidths an automatic simulation procedure was developed. The spectrum was assumed to be the superposition of eight individual derivative curves as in equation (1), where  $I_0$  is the baseline parameter,  $A$  the amplitude of the individual curves, and

$$I_{\text{calc.}}(B) = I_0 + A \sum_M F(B, B_M, \sigma_M) \quad (1)$$

$M$  the magnetic quantum number for the  $^{59}\text{Co}$  nucleus with values from  $-\frac{7}{2}$  to  $\frac{7}{2}$ . The lineshape function ( $F$ ) is

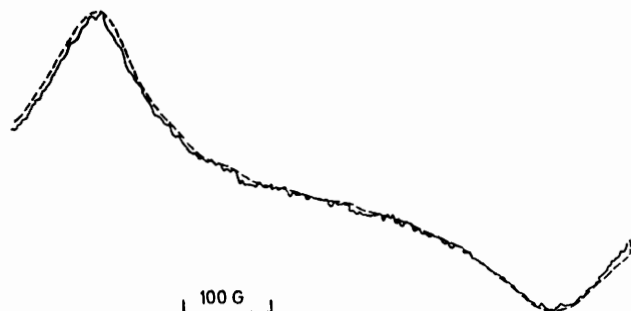


FIGURE 3 E.s.r. spectrum of  $[\text{Co}(\text{Hdmg})_2]$  in methanol solution at 60 °C. (—), Experimental, (---), calculated Lorentzian curves

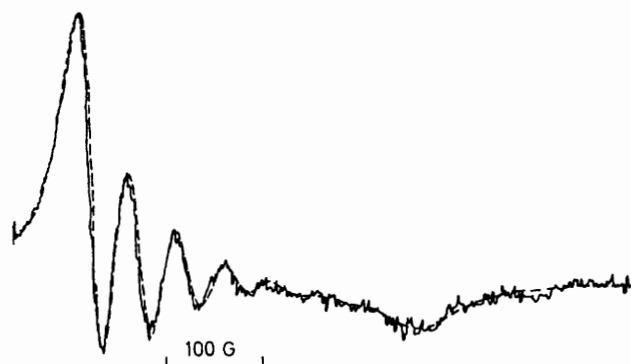


FIGURE 4 E.s.r. spectrum of  $[\text{Co}(\text{Hdmg})_2]$  in methanol solution at -24 °C. (—), Experimental, (---), calculated Lorentzian curves

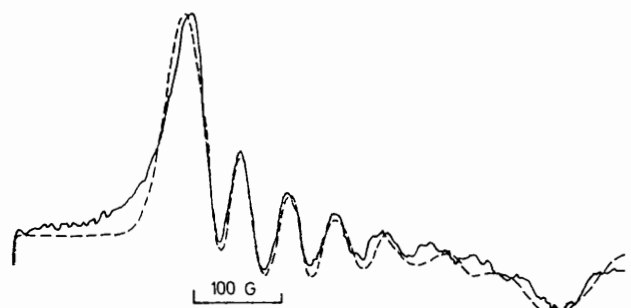


FIGURE 5 E.s.r. spectrum of  $[\text{Co}(\text{Hdmg})_2]$  in methanol solution at 2 °C. (—), Experimental, (---), calculated Gaussian curves

either a derivative Lorentzian [equation (2)], or a derivative

$$F_L(B, B_M, \sigma_M) = -(B - B_M)\sigma_M[\sigma_M^2 + (B - B_M)^2]^{-2} \quad (2)$$

Gaussian function [equation (3)], where  $B_M$  is the position

$$F_G(B, B_M, \sigma_M) = -(B - B_M)\sigma_M^{-3} \exp[-(B - B_M)^2 \ln 2 \sigma_M^{-2}] \quad (3)$$

of the line centre and  $2\sigma_M$  the linewidth at one half the maximum intensity. For an isotropic-spin Hamiltonian the position of the hyperfine lines in second order is given by equation (4). The parameters  $g_{\text{iso}}$  and  $A_{\text{iso}}$  can be determined from the simulation parameters  $B_0$  and  $B_{\text{sep}}$  according to equation (5), where  $h$  is Planck's constant,  $\beta_0$  is the Bohr magneton, and  $\omega_0$  the microwave frequency (its value in our experiments was  $5.76 \times 10^{10} \text{ s}^{-1}$ ). In the case

$$B_M = B_0 - B_{\text{sep}}M - B_{\text{sep}}^2(2B_0)^{-1}(\frac{g^2}{4} - M^2) \quad (4)$$

$$g_{\text{iso}} = h\omega_0(2\pi\beta_0 B_0)^{-1}, A_{\text{iso}} = \omega_0 B_{\text{sep}}/B_0 \quad (5)$$

of symmetrical lineshapes the number of parameters to be optimized in the curve-fitting procedure is 12; these are  $A$ ,  $I_0$ ,  $B_0$ ,  $B_{\text{sep}}$ , and the eight  $\sigma_M$  values. We also carried out calculations for asymmetrical lineshapes in which the two wings of each line are to be characterized by different  $\sigma_M$  values. This increases the number of parameters to be

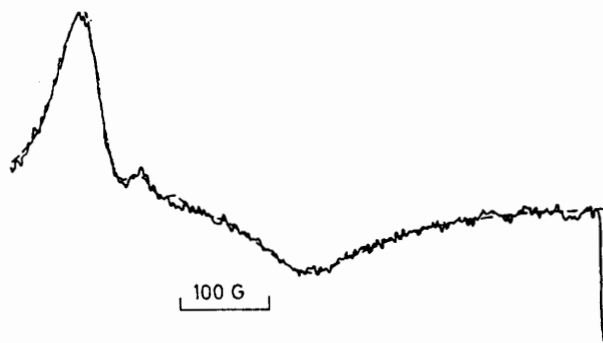


FIGURE 6 E.s.r. spectrum of  $[\text{Co}(\text{Hdmg})_2]$  in methanol solution at -60 °C. (—), Experimental, (---), calculated Lorentzian curves

optimized to 20. The fitting was made by a non-linear least-squares procedure with the iteration steps based on Meiron's formula.<sup>8</sup>

The above automatic-fitting procedure ensured convergence in *ca.* 10 steps for strongly overlapping lines. For lines with greater separation the convergence was more rapid. While the fit was very good for the Lorentzian lineshape, poor results were obtained with Gaussian lineshape (*cf.* Figures 4 and 5). The asymmetrical lineshape permits slightly better simulation than the symmetrical one; however, it can lead to loss of some of the strongly overlapping lines in the high-field part of the spectra. Therefore, we used only the data obtained from fitting by symmetrical Lorentzian curves (Table 4).

## DISCUSSION

*Interpretation of the Magnetic Parameters.*—The local symmetry of  $[\text{Co}(\text{Hdmg})_2]$  and its mixed py derivatives is  $C_{2v}$ ; however, the nearly axial  $g$  tensor corresponds to an effective  $C_{4v}$  tetragonal symmetry. The local ligand field splits the orbitally degenerate  $3d$  levels into three singlets, *viz.*  $b_2(d_{x^2-y^2})$ ,  $b_1(d_{xy})$ ,  $a_1(d_{z^2})$ , and a doublet  $e(d_{xz}, d_{yz})$ . According to Schrauzer and Lian-Pin Lee<sup>2</sup> the lack of superhyperfine interaction with the equatorial nitrogen atoms and the appearance of a superhyperfine structure due to the axial py nitrogens show that the unpaired electron is localized on the  $d_{z^2}$  orbital and the

<sup>8</sup> J. Meiron, *J. Opt. Soc. Amer.*, 1965, **55**, 1105.

electronic ground state can be given by the  ${}^2A_1(d_{x^2-y^2}, d_{z^2})$  hole-electron configuration. Ligand-field calculations of the  $g$  factors by Engelhardt and Green<sup>9</sup> support this conclusion.

The formulas of the spin-Hamiltonian parameters have been derived by taking into account the effect of the  ${}^2E(d_{x^2-y^2}, d_{xz}, d_{yz})$  excited state through spin-orbit coupling, because, among the excited states, only this gives a first-order contribution and only this state may be of such low energy that contributions of higher order are not negligible. In the molecular-orbital (m.o.) approach both the spin-orbit and hyperfine coupling constants are changed relative to their ionic values, because of the difference in shielding of the  $d$  electrons and the only partial localization of the unpaired electron on the  $d_{z^2}$  orbital. The latter effect is taken into account by introducing the reduction parameters  $k$  and  $k'$ , so that  $k^2$  and  $k'^2$  are approximately characteristic

liquid-phase spectra permit the isotropic  $g(g_{\text{iso}})$  value and the isotropic hyperfine constant ( $A_{\text{iso}}$ ) to be determined. As there is significant orbital quenching in the spectra of low-spin cobalt(II) complexes, here the higher-order contributions are neglected.

$$g_{\text{iso}} = g_0[1 + 2k^2(\lambda/\Delta E)] \quad (10)$$

$$A_{\text{iso}} = -K + P(g_{\text{iso}} - g_0) \quad (11)$$

On the basis of the hyperfine parameters, estimates can be obtained for the reduction parameter  $k'^2$  and the Fermi constant  $K$  [cf. equations (8), (9), and (11)]. For this, however, the signs of the coupling constants must be known. The large values of the cobalt hyperfine coupling constants and the large orbital contribution to  $g_{\perp}$  permit the conclusion that the unpaired electron is primarily localized on the cobalt  $3d$  orbital. Therefore, the assumption that the value of the reduction

TABLE 4

Linewidths (G) and relaxation parameters ( $10^7 \text{ rad s}^{-1}$ ) for  $[\text{Co}(\text{Hdmg})_2]$  in methanol

$\theta_c/^\circ\text{C}$	62	45	37	18	2	-20	-42	-50
$\sigma_{7/2}$	76.4	60.5	50.2	42.3	33.3	26.1	29.4	32.4
$\sigma_{5/2}$	79.4	61.4	51.5	44.3	35.6	29.9	34.8	40.0
$\sigma_{3/2}$	79.9	62.5	53.6	47.1	39.3	35.5	41.5	46.8
$\sigma_{1/2}$	81.5	65.0	55.1	50.9	43.6	42.1	48.2	53.4
$\sigma_{-1/2}$	82.6	67.5	57.9	54.4	48.9	48.9	56.5	62.0
$\sigma_{-3/2}$	86.1	71.6	60.1	60.0	54.6	57.5	66.6	76.9
$\sigma_{-5/2}$	90.5	76.5	64.0	61.4	60.5	67.8	97.2	150.3
$\sigma_{-7/2}$	96.7	77.9	68.5	68.9	66.5	85.6	134.0	275.5
$\alpha$	159.2	129.1	109.3	101.8	89.2	87.1	100.5	110.1
$\beta$	-3.06	-6.41	-4.37	-8.08	-9.98	-14.22	-15.72	-17.70
$\gamma$	0.745	0.472	0.462	0.455	0.555	1.16	1.47	3.70
$\delta$	-0.211	0.124	-0.059	0.06	0.06			
R.m.s. error	0.537	1.095	0.376	0.499	0.125	0.435	0.155	0.486

of the localization of the unpaired electron on the  $d_{z^2}$  orbital. Here  $k$  and  $k'$  may be different since the delocalization of electrons influences the spin-orbit and the hyperfine coupling constant ( $\lambda$  and  $P = g_0\beta_e g_N \beta_N \bar{r}^{-3}$ ) to different extents. Here  $g_0 = 2.0023$ , the factor of the free electron,  $\beta_N$  the nuclear magneton,  $g_N$  is the nuclear factor for  ${}^{59}\text{Co}$ , and  $\bar{r}^{-3}$  the average inverse cube of the distance between the unpaired electron and the cobalt nucleus. In order that  $k^2$  and  $k'^2$  should actually characterize delocalization, the shielding effect is taken into account separately by choosing  $\lambda$  and  $P$  to be smaller than their ionic values. Considering a number of complexes, we have found that the values of  $\lambda = 515 \text{ cm}^{-1}$  and  $P = 220 \times 10^{-4} \text{ cm}^{-1}$ , taken from Dunn<sup>10</sup> and Abragam and Pryce,<sup>11</sup> always provide acceptable  $k$  and  $k'$  values. For these conditions equations (6)–(9)

$$g_{\parallel} = g_0 [1 - \frac{3}{2}(k^2\lambda/\Delta E)^2] \quad (6)$$

$$g_{\perp} = g_0 [1 + 3k^2(\lambda/\Delta E) - 3(k^2\lambda/\Delta E)^2] \quad (7)$$

$$A_{\parallel} = -K + \frac{P}{7}[4k'^2 - (g_{\perp} - g_0) - 5(g_{\parallel} - g_0)] \quad (8)$$

$$A_{\perp} = -K + \frac{P}{7}[-2k'^2 + \frac{15}{2}(g_{\perp} - g_0) - \frac{11}{2}(g_{\parallel} - g_0)] \quad (9)$$

are obtained where  $K$  is the Fermi constant. The

parameter  $k'^2$  is between 0.5 and 1.0 seems to be justified. Using this condition as a criterion, one first determines the signs of the coupling constants and then the refined values of parameters  $k'^2$  and  $K$  can be given. When estimating the value of parameter  $k'^2$  in the five-coordinate case the  $A_{\text{iso}}$  and  $A_{\parallel}$  values were used, because in the frozen solution superposition of the spectra for various co-ordination numbers does not allow unambiguous determination of the perpendicular components. The relative signs of  $A_{\parallel}$  and  $A_{\perp}$  for the six-coordinate case have been selected so as to be consistent with the estimated upper limit for  $A_{\text{iso}}$  obtained from the liquid-phase spectrum.

Information on  $k^2$  from the  $g$  values can only be obtained if the excitation energy is known [see equations (6), (7), and (10)]. As  $k^2$  cannot differ significantly from  $k'^2$ , the value of  $\Delta E$  should be ca. 8 000–14 000  $\text{cm}^{-1}$ . Therefore, the asymmetric band observed in this range can probably be ascribed to this transition. The asymmetry in the four- and six-coordinate cases and the splitting of the line in the five-coordinate case can be interpreted either in terms of rhombic distortion or of the occurrence of the competing  ${}^2B_1 \rightarrow {}^2A_1$  transition. Therefore, the parameters  $k^2$  were evaluated by taking

<sup>9</sup> L. M. Engelhardt and M. Green, *J.C.S. Dalton*, 1972, 724.

<sup>10</sup> T. M. Dunn, *Trans. Faraday Soc.*, 1961, 57, 144.

<sup>11</sup> A. Abragam and M. H. L. Pryce, *Proc. Roy. Soc.*, 1951, A206, 173.

the centre of gravity of the lines as a basis. The approximate agreement between  $k^2$  and  $k'^2$  data seems to support the assignment of the near-i.r. band (cf. Table 5).

TABLE 5

Fermi terms and orbital-reduction factors for the [Co(Hdmg)<sub>2</sub>]-py systems

Adduct	$10^4 K / \text{cm}^{-1}$	$k^2$	$k'^2$	$\eta^2$
[Co(Hdmg) <sub>2</sub> ]	-18.8	0.978	0.721	0.0656
[Co(Hdmg) <sub>2</sub> (py)]	-3.9	0.876	0.716	0.0531
[Co(Hdmg) <sub>2</sub> (py) <sub>2</sub> ]	9.8	0.874	0.749	0.0442

The effect of co-ordination on the magnetic parameters, m.o. parameters, and on the Fermi constant can be discussed on the basis of Tables 1, 3, and 5. For isonitrilecobalt(II) complexes Maher<sup>12</sup> found that  $g_{\perp}$  and  $g_{\text{iso}}$  decrease and the Fermi term increases with increasing co-ordination number. We have observed a similar tendency in the case of the [Co(Hdmg)<sub>2</sub>(py)<sub>n</sub>] type mixed-ligand complexes. The five-co-ordinate species is, however, an exception as its  $g_{\text{iso}}$  value is slightly greater than that of the four-co-ordinate complex. This anomaly may be attributed to the effect of lower symmetry manifested through changes in the energy levels and mixing of the orbitals. At the same

time, the Fermi term changes in the 'normal' fashion, indicating that the value of  $K$  is primarily determined by the axial ligand field and is practically unaffected by the lowering of symmetry. The dependence of the Fermi term on the co-ordination number is due to direct  $3d-4s$  mixing.<sup>13</sup> As no such mixing occurs in the case of octahedral symmetry, the extent of mixing depends mainly on the tetragonal distortion, being less sensitive to further distortion. Tetragonal distortion of octahedral symmetry is extensive if the axial ligand field is weak compared with the equatorial field, significant  $3d-4s$  mixing being observed only in the case of weak axial co-ordination. To express the correlation between  $3d-4s$  mixing ( $\eta$ ) and the Fermi term ( $K$ ) in a quantitative way equation (12) has been used where  $k''$  is a reduction parameter,  $K_{\text{f.i.}}$  is the Fermi term for the free

$$K = k''^2 K_{\text{f.i.}} + \eta^2 K_{4s} \quad (12)$$

Co<sup>II</sup> ion, and  $K_{4s}$  is the isotropic hyperfine constant of a  $4s$  electron in the Co<sup>II</sup> ion. The two terms in (12) have opposite signs:  $K_{\text{f.i.}}$  is positive (according to McGarvey<sup>13</sup> its value is  $85 \times 10^{-4} \text{ cm}^{-1}$ ) and  $K_{4s}$  is negative (SCF calculations for neutral cobalt yield<sup>14</sup> a value of  $-1220 \times 10^{-4} \text{ cm}^{-1}$ ). For the Co<sup>II</sup> complexes under consideration  $K_{4s}$  is greater than this value and thus the actual extents of  $3d-4s$  mixing are smaller than those calculated in this work. However, this does not affect the trends obtained for the values of  $\eta$ . Although  $k''$  may differ from the orbital-reduction factor  $k'$ , we use the approximation  $k' = k''$  which presumably does not influence significantly the estimation of  $\eta$ . The calculated  $\eta$  values are listed in Table 5. The decrease in  $\eta$  with increasing co-ordination number is in accord with the expectation that higher co-ordination numbers imply weaker distortions of the octahedral ligand field.

In the study of the liquid-phase spectra we found that for the four-co-ordinate case the temperature exerts a strong influence on the spectrum, whereas for the five- and six-co-ordinate cases the spectra suffer only insignificant changes. The temperature dependence of

TABLE 6

Temperature dependence of magnetic parameters in the [Co(Hdmg)<sub>2</sub>]-py system

$\theta_c / ^\circ\text{C}$	$g_{\text{iso}} - g_0$	$A_{\text{iso}}$ $10^{-4} \text{ cm}^{-1}$	$K$	$A_{\parallel} - A_{\perp}^*$	$g_{\parallel} - g_{\perp}^*$
62	0.2066	65.4	-20	67.6	0.3099
45	0.2042	61.3	-16.4	68.5	0.3063
37	0.1997	59.7	-15.8	70.3	0.2996
18	0.1913	58.3	-16.1	73.6	0.2870
2	0.1887	54.5	-12.9	74.7	0.2831
-20	0.1877	51.3	-10.0	75.1	0.2816
-42	0.1824	50.6	-10.5	77.2	0.2736

\* Value calculated by comparing parameters obtained in frozen solution and in the liquid phase.

time, the Fermi term changes in the 'normal' fashion, indicating that the value of  $K$  is primarily determined by the axial ligand field and is practically unaffected by the lowering of symmetry. The dependence of the Fermi term on the co-ordination number is due to direct  $3d-4s$  mixing.<sup>13</sup> As no such mixing occurs in the case of octahedral symmetry, the extent of mixing depends mainly on the tetragonal distortion, being less sensitive to further distortion. Tetragonal distortion of octahedral symmetry is extensive if the axial ligand field is weak compared with the equatorial field, significant  $3d-4s$  mixing being observed only in the case of weak axial co-ordination. To express the correlation between  $3d-4s$  mixing ( $\eta$ ) and the Fermi term ( $K$ ) in a quantitative way equation (12) has been used where  $k''$  is a reduction parameter,  $K_{\text{f.i.}}$  is the Fermi term for the free

Co<sup>II</sup> ion, and  $K_{4s}$  is the isotropic hyperfine constant of a  $4s$  electron in the Co<sup>II</sup> ion. The two terms in (12) have opposite signs:  $K_{\text{f.i.}}$  is positive (according to McGarvey<sup>13</sup> its value is  $85 \times 10^{-4} \text{ cm}^{-1}$ ) and  $K_{4s}$  is negative (SCF calculations for neutral cobalt yield<sup>14</sup> a value of  $-1220 \times 10^{-4} \text{ cm}^{-1}$ ). For the Co<sup>II</sup> complexes under consideration  $K_{4s}$  is greater than this value and thus the actual extents of  $3d-4s$  mixing are smaller than those calculated in this work. However, this does not affect the trends obtained for the values of  $\eta$ . Although  $k''$  may differ from the orbital-reduction factor  $k'$ , we use the approximation  $k' = k''$  which presumably does not influence significantly the estimation of  $\eta$ . The calculated  $\eta$  values are listed in Table 5. The decrease in  $\eta$  with increasing co-ordination number is in accord with the expectation that higher co-ordination numbers imply weaker distortions of the octahedral ligand field.

In the study of the liquid-phase spectra we found that for the four-co-ordinate case the temperature exerts a strong influence on the spectrum, whereas for the five- and six-co-ordinate cases the spectra suffer only insignificant changes. The temperature dependence of

<sup>12</sup> J. P. Maher, *J. Chem. Soc. (A)*, 1968, 2918.  
<sup>13</sup> B. R. McGarvey, *J. Phys. Chem.*, 1967, **71**, 51.  
<sup>14</sup> E. Clementi, *J. Chem. Phys.*, 1964, **41**, 295.  
<sup>15</sup> J. J. Alexander and H. B. Gray, *J. Amer. Chem. Soc.*, 1967, **89**, 3356.  
<sup>16</sup> M. E. Kimball, D. W. Pratt, and W. G. Kaska, *Inorg. Chem.*, 1968, **7**, 2006.  
<sup>17</sup> N. Kataoka and H. Kon, *J. Amer. Chem. Soc.*, 1968, **90**, 2978.

<sup>18</sup> J. M. Assour and W. K. Kahn, *J. Amer. Chem. Soc.*, 1965, **87**, 207.

<sup>19</sup> J. M. Assour, *J. Amer. Chem. Soc.*, 1965, **87**, 4701.

<sup>20</sup> J. M. Assour, *J. Chem. Phys.*, 1965, **43**, 2477.

<sup>21</sup> H. A. O. Hill, P. J. Sadler, and R. J. P. Williams, *J.C.S. Dalton*, 1973, 1663.

<sup>22</sup> J. Danon, P. P. Muniz, A. O. Caride, and I. Wolfson, *J. Mol. Struct.*, 1967, **1**, 127.

this was permitted by the available data. The data were evaluated on the basis of the same principles used in the case of dimethylglyoximatocobalt complexes. The results obtained for pentacyanocobalt(II) and isonitrilecobalt(II) complexes are listed in Table 7, whereas the data for  $B_{12r}$ ,  $[Co(Hdmg)_2]$ ,  $Na_4[Co(pts)]$ ,  $[Co(mp)]$ ,  $[Co(pc)]$ , and  $[Co(tpp)]$  are collected in Table 8 (pts, mp, pc, and tpp = tetrasulphonated phthalocyanine, mesoporphyrin, phthalocyanine, and tetraphenylporphyrin). In Figure 7 the  $1/\Delta g = 1/(g_{iso} - g_0)$  values are plotted against  $\eta$  for all complexes considered. The complexes in Tables 7 and 8 are arranged roughly in order of  $g_{\perp}$  and  $K$ . As can be seen from these Tables and from Figure 7,  $g_{\perp}$ ,  $A_{\parallel}$ ,  $A_{\perp}$ , and  $K$  vary in the same direction.

TABLE 7

E.s.r. parameters of low-spin  $Co^{II}$  complexes with carbon donors [(1) and (13) from ref. 22, (2)–(11) from ref. 12, and (12) from ref. 15]

Complex	Solvent	$g_{\perp}$	$g_{\parallel}$	$A_{\parallel}$	$A_{\perp}$	$K$	$h'^2$	$\eta$
				$10^{-4} \text{ cm}^{-1}$				
(1) $[Co(CN)_6]^{4-}$	$K_3[Co(CN)_6]$	2.095	2.006	50.6	-68.4	42.3	0.763	0.136
(2) $[Co(CNMe)_4Cl_2]$	$CH_2Cl_2$	2.090	2.005	61.4	-73.0	41.1	0.837	0.157
(3) $[Co(CNMe)_6]^{2+}$	MeNC	2.092	2.025	61.4	-73.2	42.4	0.838	0.157
(4) $[Co(CNEt)_6]^{2+}$	EtNC	2.089		<i>a</i>	-70.2	37.4	0.849	0.169
(5) $[Co(CNC_6H_{11})_6]^{2+}$	$C_6H_{11}NC$	2.0946		58.4	-65.8	37.8	0.791	0.158
(6) $[Co(CNPh)_6]^{2+}$	CNPhNC	2.083		<i>b</i>	-72.0	39.4	0.802	0.154
(7) $[Co(CNPh)_6]^{2+}$	$H_2O$	2.0865	2.00	68.1	-68.2	35.2	0.841	0.172
(8) $[Co(CNMe)_6]^{2+}$	$CH_2Cl_2$	2.1227	2.000	72.0	-58.5	32.7	0.862	0.182
(9) $[Co(CNEt)_6]^{2+}$	$CH_2Cl_2$	2.1275	2.0064	75.0	-49.9	26.8	0.840	0.191
(10) $[Co(CNC_6H_{11})_6]^{2+}$	$CH_2Cl_2$	2.116	2.0061	73.0	-53.3	27.9	0.831	0.187
(11) $[Co(CNPh)_6]^{2+}$	$CH_2Cl_2$	2.118	2.004	80.5	-49.4	23.1	0.852	0.202
(12) $[Co(CN)_5]^{3-}$	MeOH	2.156	2.006	81.8	-28.8	14.5	0.804	0.220
(13) $[Co(CN)_5]^{3-}$	$K_3[Co(CN)_6]$	2.174	2.004	83.3	-25.4	14.4	0.820	0.213

<sup>a</sup>  $A_{iso} = -23.1$ . <sup>b</sup>  $A_{iso} = -26.9$ .

TABLE 8

E.s.r. parameters of low-spin  $Co^{II}$  complexes with nitrogen donors

Complex	Solvent	$g_{\perp}$	$g_{\parallel}$	$A_{\parallel}$	$A_{\perp}$	$K$	$h'^2$	$\eta$	Ref.
				$10^{-4} \text{ cm}^{-1}$					
(A) $B_{12r}$		2.2975	2.009	103.0	8.5	3.3	0.919	0.248	4
(B) $[Co(Hdmg)_2(py)_2]$	MeOH	2.205	2.0161	78.0	-13.0	9.8	0.749	0.210	This work
(C) $[Co(Hdmg)_2(py)]$	MeOH	2.240	2.0137	86.5	15.0	-3.9	0.716	0.230	This work
(D) $[Co(Hdmg)_2]$	MeOH	2.236	2.0106	102.0	28.6	-18.8	0.721	0.256	This work
(E) $Na_4[Co(pts)]$	$Me_2SO$	2.257	2.005	98.0	21.0	-9.7	0.766	0.248	6b
(F) $[Co(mp)]$	MeCl	2.510	2.047	97.0	81.0	-11.9	0.806	0.259	21
(G) $[Co(pc)]$	$H_2SO_4$	2.546	2.029	85.0	96.0	-12.5	0.712	0.245	19
(H) $[Co(pc)]$	$\alpha$ - $[Zn(pc)]$	2.422	2.007	116.0	66.0	-21.2	0.860	0.278	18
(I) $[Cd(pc)]$	$\beta$ - $[Zn(pc)]$	2.900	1.91	160.0	265.0	-85.0	0.764	0.351	18
(J) $[Co(tpp)]$	$H_2tpp$	2.505	2.034	115.0	92.0	-26.0	0.834	0.282	20
(K) $[Co(tpp)]$	$H_2tpp$	3.322	1.798	197.0	395.0	-106.0	0.917	0.388	20
(L) $[Co(mp)]$	$C_6H_5(NO_2)_3$	3.611	1.891	179.0	426.0	-91.7	0.884	0.370	21

There is a correlation in Figure 7 between the position of the individual complexes and the axial ligand field: the six-co-ordinate isonitrile complexes are in the upper left corner, the five-co-ordinate species being below them. It is noteworthy that in the middle of the Figure,  $[Co(Hdmg)_2]$  and  $B_{12r}$  are very closely located, supporting the view that  $[Co(Hdmg)_2]$  may be regarded as a vitamin  $B_{12r}$  model compound. The lower right corner includes solid complexes with very weak axial ligand field. As the axial field in the solid state is determined by the crystal lattice the appreciable differences between various modifications can be readily interpreted.

According to Figure 7 a linear correlation exists between the extent of  $3d-4s$  mixing ( $\eta$ ) and  $1/\Delta g$  for the complexes studied: all points fall on a straight line with the only exception of a  $[Co(pc)]$ ,  $[Co(tpp)]$ , and  $[Co(mp)]$  centre. The observed linearity may be attributed to an approximately linear dependence of both parameters on the axial distortion of the local octahedral ligand field. The extent of  $3d-4s$  mixing ( $\eta$ ) depends on  $\langle 3d|V_{tetragonal}|4s \rangle$  and on the energy separation between the  $3d^6 4s$  and the  $3d^7$  configurations. For the free  $Co^{II}$  ion this energy separation is  $46\,000 \text{ cm}^{-1}$ ; <sup>23</sup> its value for the complexes in question may differ from this but must be approximately constant within the series. Therefore,  $\eta$  is proportional to the tetragonal distortion of the octahedral ligand field. On the other

hand,  $1/(g_{iso} - g_0)$  is proportional to the  ${}^2E-{}^2A_1$  energy separation. According to the ligand-field calculations of Engelhardt and Green,<sup>9</sup> the  ${}^2E-{}^2A_1$  separation is large for strong axial ligand fields and *vice versa*, *i.e.* the energy separation is roughly proportional to the strength of the axial ligand field. This proportionality implies a linear relation between the distortion of the octahedral ligand field and  $1/(g_{iso} - g_0)$ . In the case of very weak axial ligand fields this probably ceases to be true, explaining the anomalous behaviour of one of the  $[Co(pc)]$ ,  $[Co(tpp)]$ , and  $[Co(mp)]$  centres.

<sup>23</sup> C. E. Moore, 'Atomic Energy Levels,' Nat. Bureau Stand., 1958.

The data in Tables 7 and 8 show that the orbital-reduction parameter  $k'^2$  varies in a rather narrow interval (0.712–0.862). This lends support to the correctness of the selection of the signs of the hyperfine constant and to the correct magnitude of parameters  $P$  and  $\lambda$ . On the other hand the near constancy of  $k'$

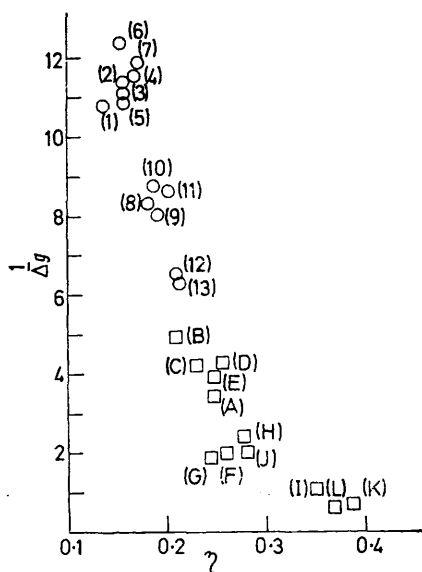


FIGURE 7 Correlation between  $1/\Delta g$  and the extent of  $3d-4s$  mixing for low-spin  $\text{Co}^{\text{II}}$  complexes (the letters and numbers are those given in Tables 7 and 8)

indicates that delocalization of the unpaired electron is but slightly affected by changes in the nature of the equatorial ligands.

A more direct estimate for the delocalization can be obtained from the superhyperfine constants. Using the results of Maki and McGarvey<sup>24</sup> we obtain delocalization of  $\epsilon_2^2 = 0.1$  for  $[\text{Co}(\text{Hdmg})_2(\text{py})]$  and  $\epsilon_2^2 = 0.2$  for  $[\text{Co}(\text{Hdmg})_2(\text{py})_2]$ . This contradicts our observation that the reduction parameter  $k$  shows no significant differences between these two complexes. This discrepancy may be due either to the arbitrary assignment of the  ${}^2E-{}^2A_1$  transition, to the rather complex correlation<sup>25</sup> between the delocalization and the reduction parameter  $k$ , or to enhanced delocalization of the unpaired electron onto the methanol molecule occupying the sixth co-ordination site in  $[\text{Co}(\text{Hdmg})_2(\text{py})]$ .

If one assumes that the narrowest hyperfine line in the spectrum of  $[\text{Co}(\text{Hdmg})_2]$  in frozen solution is an unresolved superposition of the superhyperfine structure due to the four equatorial nitrogens, an interesting correlation can be obtained between the axial and equatorial delocalization of the unpaired electron. A slight equatorial delocalization is conceivable as the  $d_{xy}$  orbital has a small lobe in the  $xy$  plane. This assumption is supported by the fact that the shape of the fourth line in the parallel hyperfine structure can be remarkably well fitted with the envelope of a

<sup>24</sup> A. H. Maki and B. R. McGarvey, *J. Chem. Phys.*, 1958, **29**, 35.

<sup>25</sup> M. Gerloch and J. R. Miller, *Progr. Inorg. Chem.*, 1968, **10**, 1.

1 : 4 : 10 : 16 : 19 : 16 : 10 : 4 : 1 multiplet corresponding to four equivalent nitrogen atoms (Figure 8). The superhyperfine constants obtained by this fitting procedure are  $2.5 \times 10^{-4} \text{ cm}^{-1}$  for  $[\text{Co}(\text{Hdmg})_2]$  and  $1.75 \times 10^{-4} \text{ cm}^{-1}$  for  $[\text{Co}(\text{Hdmg})_2(\text{py})_2]$ . Consequently, a higher axial delocalization is associated with a lower equatorial delocalization of the unpaired electron. The same phenomenon has been observed by Falk *et al.*<sup>26</sup> in the case of  $[\text{Cu}(\text{Hdmg})_2]$ .

*Interpretation of Linewidth Data.*—The parameters of equation (13) proposed by Wilson and Kivelson<sup>27</sup> were

$$\sigma_M = \alpha + \beta M + \gamma M^2 + \delta M^3 \quad (13)$$

fitted to the linewidth data by a least-squares procedure. Since at low temperatures the outermost lines in the high-field part are very broad, at  $-20^\circ \text{C}$  only seven, whereas at and below  $-42^\circ \text{C}$  only six, linewidths were taken into account (the linewidths are neglected when  $\sigma_M$  is greater than twice the hyperfine separation). Parameters  $\alpha$ ,  $\beta$ ,  $\gamma$ , and  $\delta$  and the linewidth data obtained by the simulation procedure are listed in Table 4.

The evaluation is based on the formulae of Wilson and Kivelson,<sup>27</sup> with the assumption of axial symmetry. As  $g_{\text{iso}}$  and  $A_{\text{iso}}$  depend on the temperature, the temperature dependence of the anisotropic parameters

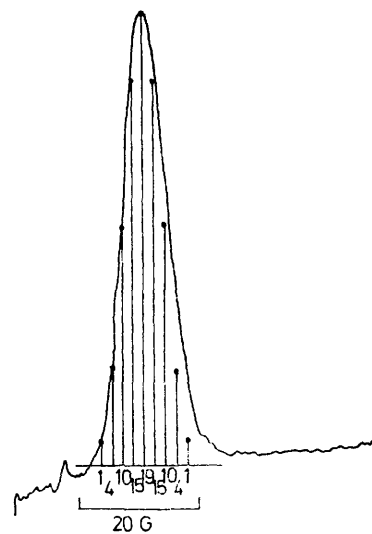


FIGURE 8 Part of the  $[\text{Co}(\text{Hdmg})_2]$  e.s.r. spectrum on frozen methanol: fourth line of the cobalt hyperfine structure in parallel orientation; the assumed but unresolved superhyperfine structure of in-plane nitrogen atoms is also shown

should also be taken into account as a correction (Table 4). Assuming that the temperature dependence of the parameters is due to changes in the excitation energy,

$$(g_{\perp} - g_{\parallel})_T = 1.5(g_{\text{iso}} - g_0)_T \quad (14)$$

$$(A_{\perp} - A_{\parallel})_T = (A_{\perp} - A_{\parallel})_{\text{LN}} + 1.82(g_{\text{iso},T} - g_{\text{iso,LN}}) \quad (15)$$

<sup>26</sup> R. E. Falk, E. Ivanova, B. Roos, and T. Vännngard, *Inorg. Chem.*, 1970, **9**, 556.

<sup>27</sup> R. Wilson and D. Kivelson, *J. Chem. Phys.*, 1966, **44**, 154.

equations (14) and (15) can be obtained where the subscripts  $T$  and LN refer to the actual and to liquid-nitrogen temperature. We assume that the Debye theory of rotational relaxation is applicable in the present case and the correlation time,  $\tau_R$ , is given by equation (16),<sup>28</sup> where  $\eta$  is the coefficient of viscosity and  $r$  the radius of the equivalent rotating sphere. The  $\eta$  values for methanol at different temperatures have been taken from ref. 29. It follows from equation (16)

$$\tau_R = 4\pi\eta r^3/3kT \quad (16)$$

that the relaxation parameters should be proportional to  $\eta/T$ . This is true in the case of  $\beta$  and  $\gamma$ , but  $\alpha$  reveals a minimum at *ca.*  $-20^\circ\text{C}$ . The best fit for the  $\beta$  values was obtained with  $r = 3.6 \text{ \AA}$ , which also gave a satisfactory fit for the  $\gamma$  values (Table 9). Although the fit is poorer at the highest and lowest temperatures, it is still acceptable as under these conditions the hyperfine structure practically collapses into a single broad line.

molecular radius estimated from X-ray data in the case of [VO(pd)] (pd = pentane-2,4-dionate), although the Debye radius was somewhat smaller than expected. The better agreement in the present system is due probably to the fact that the conditions required for the Debye theory to be valid are satisfied to a better approximation for [Co(Hdmg)<sub>2</sub>] in methanol than for [VO(pd)] in benzene. More specifically, the size of the methanol molecule relative to that of [Co(Hdmg)<sub>2</sub>] ensures that the solvent can be regarded as a viscous continuum whereas this is not true to the same extent for the benzene solution of [VO(pd)].<sup>32</sup>

To check the validity of the assumption underlying equation (17), we estimated the rotational-correlation<sup>28</sup> time from (18), where  $I$  is the molecular moment of

$$\tau_\omega = I/8\pi r^3\eta \quad (18)$$

inertia. X-Ray data for [Ni(Hdmg)<sub>2</sub>]<sup>31</sup> were used to calculate the moment of inertia for the tetragonal axis,

TABLE 9

Relaxation parameters and correlation times for [Co(Hdmg)<sub>2</sub>] in methanol \*

$\theta_c/^\circ\text{C}$	$\alpha'$	$\alpha''$	$10^{-7} T_2^{-1}/$ rad s <sup>-1</sup>	$\beta$	$\gamma$	$\eta T^{-1}/P K^{-1}$	$10^{10}\tau_R/s$	$10^{14}\tau_\omega/s$
62	14.5	144.7	153.0	-4.46	0.235	1.04	0.1476	9.75
45	17.1	112.0	116.0	-5.30	0.288	1.35	0.1917	7.90
37	18.3	91.0	98.4	-5.85	0.332	1.52	0.2213	7.22
18	21.4	80.4	65.7	-7.11	0.449	2.08	0.2955	5.60
2	26.6	62.6	46.0	-9.09	0.601	2.88	0.409	4.28
-20	39.0	48.1	28.2	-13.5	0.930	4.67	0.654	2.88
-42	64.2	36.3	15.1	-23.0	1.703	8.23	1.17	1.79
-50	83.1	27.0	11.0	-30.4	2.31	11.0	1.56	1.39

\* For anisotropic relaxation  $r = 3.6 \text{ \AA}$  and for spin-rotational relaxation  $r = 3.5 \text{ \AA}$ .

The calculated  $\delta$  values are smaller than  $10^5 \text{ s}^{-1}$ ; consequently this contribution to the linewidth can be neglected.

By calculating  $\alpha'$  from the relaxation formulas<sup>27</sup> and subtracting it from the measured value of  $\alpha$  one obtains the 'residual linewidth,'  $\alpha''$ . Since  $\alpha''$  shows good linearity with  $T/\eta$ , the major contribution to the residual linewidth is from spin-rotational relaxation. According to Atkins and Kivelson,<sup>30</sup> if the correlation time for re-orientation is much greater than for rotation the spin-rotational relaxation time is given approximately by equation (17), where  $\Delta g_{\parallel}$  and  $\Delta g_{\perp}$  are the differences

$$T_2^{-1} = (12\pi r^3)^{-1}(\Delta g_{\parallel}^2 + 2\Delta g_{\perp}^2)kT/\eta \quad (17)$$

between the corresponding  $g$  values and that for the free electron. The best fit between  $T_2^{-1}$  and  $\alpha''$  was obtained with  $r = 3.5 \text{ \AA}$  (Table 9). The excellent agreement between the radii calculated from the two different relaxation mechanisms and the molecular radius of [Ni(Hdmg)<sub>2</sub>] based on X-ray data<sup>31</sup> supports the correctness of the Debye model in the present system. Wilson and Kivelson<sup>27</sup> also found satisfactory agreement between the effective Debye radius and the

the result being  $I = 3.5 \times 10^{-37} \text{ g cm}^2$ . The correlation time  $\tau_\omega$  obtained with this value is three to four orders of magnitude smaller than  $\tau_R$ . The calculated relaxation parameters, the correlation times, and  $\eta/T$  values are listed in Table 9.

#### EXPERIMENTAL

The e.s.r. spectra were recorded on a JES-ME-3X type spectrometer in X band with a field modulation of 100 kHz. The magnetic field was measured with a JES-FC-1 proton-field calibrator unit. For the measurement of  $g$  values a Mn-MgO probe was employed. The spectra were digitalized using a JRS-5 analogue-digital converter and the calculations were made on a CDC 3300 computer. Solution e.s.r. spectra were recorded between  $-60$  and  $+60^\circ\text{C}$ . The temperature was controlled by a copper-constantan thermocouple. Spectra of frozen solutions were recorded at liquid-nitrogen temperature.

Samples were prepared in an atmosphere of argon. As the solvent was methanol, solution spectra were recorded in calibrated capillaries. The concentration of the complex was varied between 0.5 and 10 mmol dm<sup>-3</sup>, and that of pyridine in the interval 0–8.0 mol dm<sup>-3</sup>. In order to maintain a nearly identical sensitivity at a given temperature, the same radio-frequency power of *ca.* 10 mW

<sup>28</sup> N. Blombergen, E. W. Purcell, and R. V. Pound, *Phys. Rev.*, 1948, **73**, 679.

<sup>29</sup> 'Handbook of Chemistry and Physics,' ed. R. C. Weast, The Chemical Rubber Co., Cleveland, 1970–1971.

<sup>30</sup> P. W. Atkins and D. Kivelson, *J. Chem. Phys.*, 1966, **44**, 169.

<sup>31</sup> K. Nakamoto and P. J. McCarthy, 'Spectroscopy and Structure of Metal Chelate Compounds,' John Wiley and Sons, Inc., New York, 1968.

<sup>32</sup> A. Spornol and K. Wirtz, *Z. Naturforsch.*, 1953, **A8**, 522.



incident on the cavity and the same modulation amplitude of 5 G was used throughout, except in the case of frozen solutions.\* A Mn-MgO standard was applied to correct for the sensitivity differences.

\* 1 G =  $10^{-4}$  T.

Electronic absorption spectra were recorded at room temperature on a Unicam SP 700 instrument in the near-i.r. and on a Hitachi-Perkin-Elmer 124 spectrometer in the visible and u.v. regions.

[3/881 Received, 25th April, 1973]

---